

Calculation Method of Instantaneous Wind Speed Spatial Distribution of Wind Farm

<http://dx.doi.org/10.3991/ijoe.v11i1.4157>

Gu Bo, Hu Hao, Huang Hui and Liu Xinyu

North China University of Water Resources and Electric Power, Zhengzhou, China

Abstract—Instantaneous wind speed spatial distribution of wind farm is the basis of the optimal control for wind turbines. A calculation method was proposed for the instantaneous wind speed spatial distribution in wind farm, which made the instantaneous wind speed spatial distribution is divided into wake and non-wake zone. For the non-wake zone, the instantaneous wind speed spatial distribution is mainly affected by the flow field coupling between wind turbines, in order to describe the influence accurately, a cross spectral matrix was constructed including the wind turbine mutual distance and the azimuth in wind farm, and the solving calculation process of the cross spectral matrix was deduced. For the wake zone, single wind turbine wake model and wake superposition model were established according to conservation of momentum, and then the average wind speed spatial distribution in wake zone was calculated. According to the average wind speed spatial distribution, the instantaneous wind speed spatial distribution was calculated. A wind farm is selected as case to verify the calculation method, and the results show that this calculation method can accurately describe the instantaneous wind speed spatial distribution of wind farm.

Index Terms—Wind Farm; Wind Turbines; Power Spectral Density; Cross Spectral Matrix; Wake

I. INTRODUCTION

At the end of 2012, Chinese total installed capacity of wind power has reached 7,641MW, ranking first in the world. In terms of capacity and power generation, wind power has become the third largest main power supply after thermal power and hydroelectric power in Chinese electric system, and will continue to grow over the next ten years. Incompatible with this, there is still a wide gap between Chinese wind power technology and the international advanced level.

Wind speed distribution characteristics are the basis of the wind farm optimal control, and the study of wind speed distribution in wind farms has extensive theoretical and practical value. Using radar technology and vector retrieval method, the wind speed distribution, wind direction and air density etc., can be accurately measured [1]. The radar technology used in wind speed measurements in complex terrain is in-depth studied, the results show that under the moderately complex terrain condition, the radar measurement error is 3-4%, and in complex terrain condition, the radar measurement error up to 10% [2]. In order to design the wind turbine of safety and economical operation in the hilly environment, the flow field characteristics of hills was studied in wind tunnel, as well as the wake characteristics of single double-fed wind turbine and the wake interference of multi double-fed wind turbines were studied in wind tunnel, these study results are used to

support the design and economic operation of double-fed wind turbines in complex terrain [3]. The wake characteristics of doubly-fed wind farm were studied using CFD software in complex terrain in [4-5], and the comparative analysis about the wake characteristics of doubly-fed wind farm in complex terrain and flat terrain was performed. The flow field characteristics of doubly-fed wind farm also were studied using CFD software in complex terrain in [6-8], and the main purpose of the study is to comprehend the turbulence characteristics of doubly-fed wind farm. In order to study the randomness and turbulence characteristics of wind speed, the spectrums of the randomness wind speed is analyzed from the perspective of the frequency domain, and the correlation function is used to describe the turbulence effects between different positions in flow field [9-12].

Accurate description of the wind speed characteristics when rotor is rotating is the basis of study the double-fed wind turbine fatigue load and power fluctuation. Therefore, the wind speed model based on correlation function was in-depth studied, the model can relatively accurate describe the wind characteristics in the process when rotor is rotating [13-17]. The authors above have studied the wind speed characteristics of wind farm from different angles. Field measurements and wind tunnel experiments can get accurate data, but they require expensive test equipments and a large number of test time, it cannot meet the requirements of double-fed wind farm optimization control for real-time. Using CFD software to calculate the flow field also can meet certain requirements in accuracy, but it requires a lot of computation time too, it also cannot meet the requirements of double-fed wind farm optimization control for real-time. The wind speed calculation model of single double-fed wind turbine based on the frequency domain, whose calculation time is short and calculation accuracy is high. However, the study mainly focuses on single double-fed wind turbine, and few studies have been studied for the entire wind farm.

Based on the current research status, a calculation method was proposed for the instantaneous wind speed spatial distribution in wind farm, which divide the instantaneous wind speed spatial distribution into wake zone and non-wake zone. For the non-wake zone, a cross spectral matrix was constructed including the wind turbine mutual distance and the azimuth in wind farm, and the solving calculation process of the cross spectral matrix was deduced. For the wake zone, wake model and wake superposition model were established according to conservation of momentum, and then the average wind speed spatial distribution in wake zone was calculated. According to the average wind speed spatial distribution, the instantaneous wind speed spatial distribution was calcu-

lated. A wind farm is selected as case to verify the calculation method.

II. NATURAL WIND SPECTRUM

The neural wind speed can be represented by equation (1).

$$\begin{cases} U = \bar{U}(z) + u(y, z, t) \\ v = v(y, z, t) \\ w = w(y, z, t) \end{cases} \quad (1)$$

In the equation (1), $\bar{U}(z)$ is the longitudinal average wind speed of a point in the flow field, u is the longitudinal fluctuating wind speed, v is the lateral fluctuating wind speed; w is the vertical fluctuating wind speed.

Under the condition of neutral atmosphere, without considering the Coriolis effect, the longitudinal average wind speed $\bar{U}(z)$ can be obtained by equation (2).

$$\bar{U}(z) = \frac{u_*}{k} \ln(z/z_0) \quad (2)$$

In the equation (2), u_* is the friction velocity, k is the von Karman constant, z_0 is the surface roughness. Under the condition of neutral atmosphere, the value of k is 0.4.

Due to the fluctuating wind velocity of the natural wind have random characteristics, so the changes of the three fluctuating wind speeds are independent of each other, which can be described by wind speed spectrum. The Von Karman spectrum and the Kaimal spectrum are commonly used wind speed spectrum. The slope of the Kaimal spectrum changes greatly in the low-frequency part, thus the Kaimal spectrum can more accurately describe the turbulence characteristics of wind. In this paper, the Kaimal spectrum is used to describe the fluctuating wind speed. The spectrum representation of three fluctuating wind speed can be represented by equation (3), equation (4) and equation (5).

$$S_u(f) = u_*^2 \frac{52.5(z/\bar{U}(z))}{(1+33(z/\bar{U}(z))f)^{5/3}} \quad (3)$$

$$S_v(f) = u_*^2 \frac{8.5(z/\bar{U}(z))}{(1+9.5(z/\bar{U}(z))f)^{5/3}} \quad (4)$$

$$S_w(f) = u_*^2 \frac{1.05(z/\bar{U}(z))}{1+5.3((z/\bar{U}(z))f)^{5/3}} \quad (5)$$

Figure 1 shows the results of the three fluctuating wind spectrum, the calculation parameters of the figure, respectively is $\bar{U}(z) = 12ms^{-1}$, $z = 70m$, $u_* = 1.78ms^{-1}$, $z_0 = 0.0054m$.

For optimization control of wind farms, the longitudinal distribution of wind speed plays a decisive role, so this paper focuses on the longitudinal distribution of wind speed. Selecting an actual wind farm as the study case, the wind farm contains 20 wind turbines, the X-axis direction length of wind farm is 4500m, and the length of Y-axis direction is 5500m, the distribution of wind turbines is shown in figure 2. Figure 3 is the X-axis velocity distribution of the longitudinal fluctuating wind speed calculated by Kaimal power spectral density.

A. Cross-spectral matrix

In wind farm, the upstream wind turbines will impact on the wind speed of the downstream wind turbines. The wind speed related phenomena between the wind turbines is shown in figure 4. Where d_{rc} is the distance between the r and the c wind turbine, θ_{rc} is the angle of the north direction and the line that connects the r and the c wind turbine, θ_v is wind angle, α_{rc} is the angle between wind

direction, $\bar{U}(t)$ is the average wind speed in flow field, τ_{rc} is the time of the wind flow from the wind turbine r to the wind turbine c . The equation of τ_{rc} is as follow:

$$\tau_{rc} = \frac{\cos(\alpha_{rc}) \cdot d_{rc}}{\bar{U}(t)} \quad (6)$$

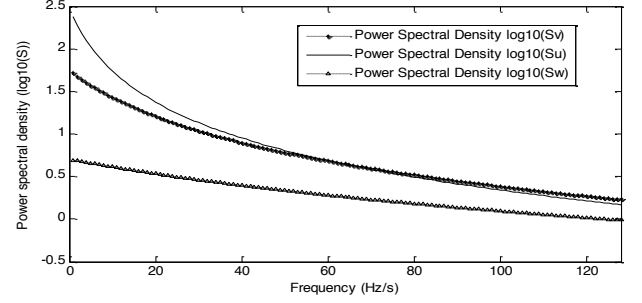


Figure 1. Kaimal power spectral density of fluctuating wind speed

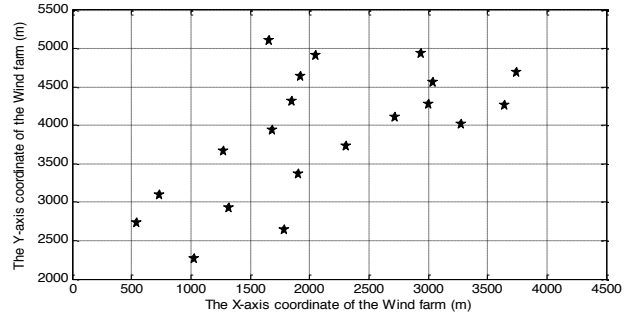


Figure 2. The distribution map of wind turbine

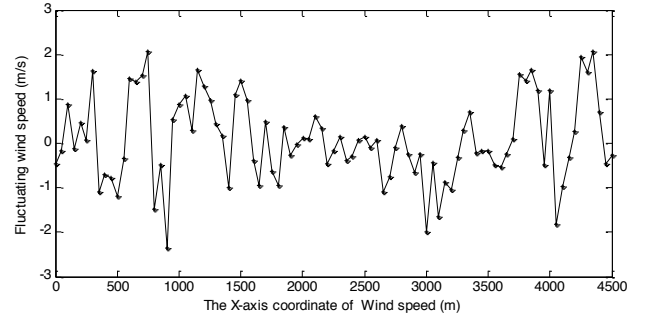


Figure 3. Fluctuating wind speed distribution in X-axis direction

III. THE COUPLING RELATIONSHIP BETWEEN WIND TURBINES

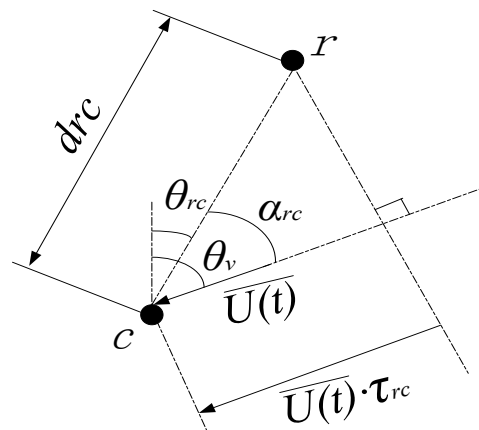


Figure 4. The coupling relationship between wind turbines

According to the definition, the correlation function about the turbulent wind speed of any two wind turbines can be obtained as shown in equation (7).

$$R_{rc}(\tau_{rc}) = E\{v_{hub,r}(t) \cdot v_{hub,c}(t - \tau_{rc})\} \quad (7)$$

In the equation (7), $v_{hub,r}(t)$ and $v_{hub,c}(t)$ are the turbulent wind speed of the r and the c wind turbine at hub height, $E\{f(t)\}$ represents the mean time within t .

The Fourier transform of $R_{rc}(\tau_{rc})$, the frequency domain functions of the correlation function can be shown as equation (8), the correlation function is the wind turbines r and c turbulent wind speed.

$$S_{rc}(f) = \int_{-\infty}^{+\infty} R_{rc}(\tau_{rc}) e^{-j2\pi f \tau_{rc}} dt \quad (8)$$

The plural form of the equation (8) is shown as equation (9).

$$S_{rc}(f) = |S_{rc}(f)| \cdot e^{-j2\pi f \tau_{rc}} \quad (9)$$

Supposing there are N wind turbines in the wind farm at present, according to equation (8) the cross spectrum matrix of the whole wind farm can be expressed as equation (10).

$$S(f) = \begin{bmatrix} S_{11}(f) & S_{12}(f) & \cdots & S_{1N}(f) \\ S_{21}(f) & S_{22}(f) & \cdots & \cdots \\ \vdots & \vdots & \ddots & \vdots \\ S_{N1}(f) & S_{N2}(f) & \cdots & S_{NN}(f) \end{bmatrix} \quad (10)$$

In the equation (10), $S_{rr}(f)$ is turbulence autocorrelation spectrum of the wind turbine r , which is real; $S_{rc}(f)$ is cross-correlation spectrum of turbulence wind speed between the wind turbine r and the wind turbine c , the cross-correlation spectrum is complex. The cross power spectrum matrix is a symmetric and nonnegative matrix.

A. Cross spectral matrix calculation

The cross spectral matrix (10) is continuous, in the use of computer calculation processing, it must be discretized. Assuming that the time of wind speed calculation is T_p , frequency f is discretized into $\Delta f = 1/T_p$, the i th discrete point corresponding to the frequency value is $f_i = i \cdot \Delta f$, and the $S_{rc}(f)$ corresponding to the discrete value is $S_{rc}(i) = S_{rc}(f_i) \cdot \Delta f$.

In addition to discretize the frequency, the sampling time is also need to be discretized. Assuming the sampling frequency is f_s , then $\Delta t = 1/f_s$ is the sampling interval, sampling frequency range is $\pm f_s/2$, the corresponding sampling points, respectively are $\pm N_s/2$ and $N_s = T_p \cdot f_s$. N_s represents the number of sampling times. In order to use the fast Fourier transform (FFT) to improve the calculation speed, N_s may be chosen to be a multiple of 2.

The Cholesky decomposition is used on the discretized cross spectral power matrix $S(i)$, the expression can be shown as equation (11) after decomposed.

$$S(i) = H(i)H^{*T}(i) \quad (11)$$

It is can be known from the nature of Cholesky decomposition, $H(i)$ is a lower triangular matrix, the diagonal elements can be solved according to equation (12).

$$H_{rr}(i) = \sqrt{S_{rr}(i) - \sum_{k=1}^{r-1} H_{rk}(i)H_{rk}^*(i)} \quad (12)$$

Non-diagonal elements can be solved according to the equation (13).

$$H_{rc}(i) = \frac{S_{rc}(i) - \sum_{k=1}^{c-1} H_{rk}(i)H_{ck}^*(i)}{H_{cc}(i)} \quad (13)$$

It is can be seen that $H(i)$ and $S(i)$ have the same phase angle from equation (12) and (13), that the phase angle of diagonal elements is 0, the phase angle of lower triangular elements is $-2\pi f \tau_{rc}$.

Since $S_{rc}(-i) = S_{rc}^*(i)$, in the calculation processing, only the part spectral values $i \geq 0$ need to be calculated. For each frequency value f_i of $i \geq 0$, a $N \times 1$ vector $E(i)$ is generated randomly according to equation (14).

$$E(i) = e^{j\varphi(i)} \quad (14)$$

In equation (14), $\varphi(i)$ is a $N \times 1$ vector whose element value distribution is in $[0; 2\pi]$. Thus the wind speed of frequency f_i can be calculated as follow:

$$U_{hub}(i) = H_{hub}(i)E(i) \quad (15)$$

The wind speed spectrum discrete series $U_{hub,r}(i)$ of the wind turbine r are combined into an array $U_{hub,r}$, then the $U_{hub,r}$ is for an inverse Fourier transform, and the wind speed $u_{hub,r}(t)$ after the wind turbine r can be obtained, the wind speed $u_{hub,r}(t)$ includes the turbulence related information between wind turbines, and the wind flow time is T_p .

According to the cross spectral matrix described in this section, the fluctuating wind speed of the wind farm in non-wake zone is calculated, the results are shown in Figure 5. The solid line is natural wind fluctuating wind speed distribution in X-axis according to the Kaimal power spectral density. The dotted line is the fluctuating wind speed of non-wake zone distribution in X-axis which considering the coupling relationship between wind turbines. It is can be seen from the figure that the distribution characteristics of the fluctuating wind speed are significantly different between considering the coupling relationship and not considering. This indicates that wind speed distribution of wind farm is affected by the coupling relationship between wind turbines.

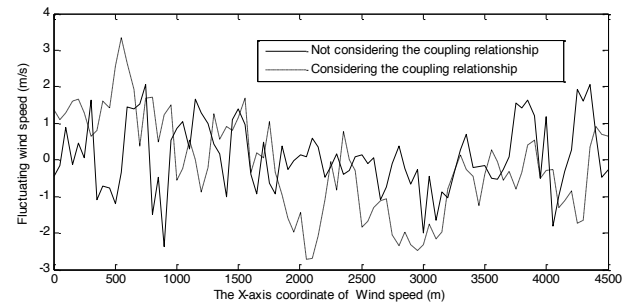


Figure 5. Fluctuating wind speed chart

Figure 6 is a fluctuating wind statistical chart. The solid line is the fluctuating wind speed statistics considered the coupling relationship between wind turbines. And the dotted line is fluctuating wind speed statistics calculated by Kaimal power spectral density. From the figure, two fluctuating wind speed follow normal distribution, mean value coordinates are basically the same, but due to the influence of the coupling relationship between wind turbines, the variances of the fluctuating wind speed is different.

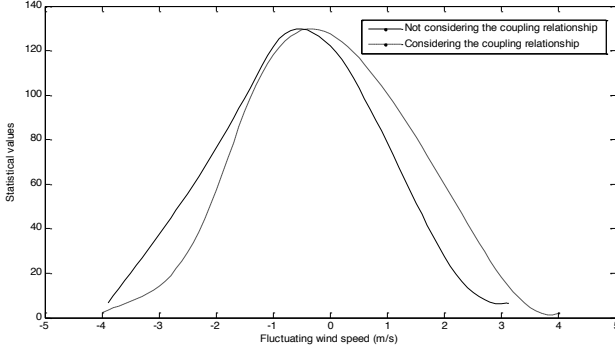


Figure 6. The statistical feature of fluctuating wind

IV. WIND FARM WAKE MODEL

A. The single wind turbine wake model

Figure 7 is the schematic diagram of the fluid flowing through the wind turbine. U_0 is the inflow wind speed, D_0 is the rotor diameter of wind turbine, A is the wake area from the distance x of wind turbine, U is the flow speed in wake region. Assuming that there is a cylinder existing outside the wind turbine flow lines, as the dotted line shown in Figure 7, V is the volume of the cylinder, A_T is the surface area of the cylinder. All the planes of the cylinder do not interactive with the outside fluid expect for the import and export plane.

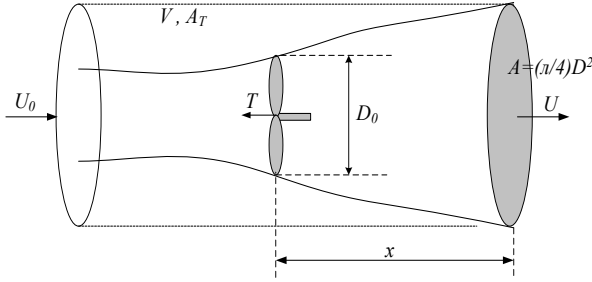


Figure 7. The control body when fluid flowing through the wind turbine

In the cylinder, according to the momentum conservation theory the equation (16) can be derived.

$$\int_V \rho \frac{\partial \vec{U}}{\partial t} dV + \int_{A_T} \rho \vec{U} (\vec{U} dA) = - \int_{A_T} p dA + \int_V \rho g dV + T + \int_{A_T} \tau dA \quad (16)$$

Assuming that the cylinder is long enough, the inlet plane and the outlet plane of the cylinder are in the stable state with the flow field outside. Under low wind speed, the air flow can be regarded as inviscid flow. The first term on the left in equation (16) is equal to 0, and the first, the second and the fourth term on the right are also equal to 0. So the equation (16) can be simplified to equation (17).

$$T = \int_A \rho U (U_0 - U) dA = \rho U (U_0 - U) A \quad (17)$$

According to the aerodynamic principle, the thrust acting on the wind turbine can be expressed as equation (18).

$$T = \frac{1}{2} \rho A_0 U_0 C_T \quad (18)$$

In the equation, A_0 is the swept area of the wind turbine, C_T is the thrust coefficient of the wind turbine. Simultaneous equation (17) and (18), the equation (19) can be derived.

$$\frac{A}{A_0} = \frac{1-a/2}{1-a} \quad (19)$$

In equation (19), a is the axial induction. The relationship between the axial induction factor and thrust coefficient can be expressed as equation (20).

$$C_T = a(2-a) \Rightarrow a = 1 - \sqrt{1-C_T} \quad (20)$$

Simultaneous equation (19) and (20), the relationship between the cross-sectional area in wake and the swept area of the wind turbine can be expressed as formula (21).

$$A = \beta A_0, \quad \beta = \frac{1}{2} \frac{1 + \sqrt{1-C_T}}{\sqrt{1-C_T}} \Rightarrow D = \sqrt{\beta} D_0 \quad (21)$$

It can be known from the equation (21), that the expansion of the wake region indicates a non-linear variation.

The equation (17), (18), (19) and (20) shown that the relationship between the wake wind speed U and inflow wind speed can be obtained as equation (22).

$$\frac{U}{U_0} = \frac{1}{2} \pm \frac{1}{2} \sqrt{1 - 2 \frac{A_0}{A} C_T} \quad (22)$$

If $a \leq 0.5$, the right side of equation (22) takes "+", and if $a > 0.5$, then takes "-". As the value of axial induction factor of wind turbine is usually less than 0.5, the equation (23) can be derived.

$$\frac{U}{U_0} = \frac{1}{2} + \frac{1}{2} \sqrt{1 - 2 \frac{A_0}{A} C_T} \approx 1 - \frac{1}{2} \frac{A_0}{A} C_T \approx 1 - a \frac{A_0}{A} \quad (23)$$

The wind tunnel experiment and field test have been conducted for far wake field in [15], the nonlinear change process of the far wake field wake radius with the changing distance has been further amended, and then the equation (24) can be obtained.

$$D(x) = (\beta^2 + \alpha s)^{\frac{1}{k}} D_0, \quad s = x / D \quad (24)$$

In equation (24), x represents the distance from a certain point in far wake to the wind turbine, the value of α should be obtained by experiment.

It can be known from the reasoning process above that the change of the radius in far wake region and the wake velocity is nonlinear and changes with the distance. The nonlinear model of the flow velocity and the radius of the far wake region have been built in this paper according to the equation (23) and (24).

B. The wake superposition model

The downstream wind turbine will suffer the wake effect from the different locations of upstream wind turbines, this phenomenon is called wake superposition, the relationship of the wake from the different location upstream wind turbine include disjointness, partial overlap-

ping and completely containing three cases, as shown in figure 8 and 9.

According to the wake superposition model provided in paper [16] and the single unit wake model as said above, the equation (25), (26), and (27) can be derived from equation (23) and (24).

$$U_j = U_i \left(1 - \frac{1}{2} \frac{A_0}{A} C_T\right) = U_i \left(1 - \frac{1}{2(\beta^{k/2} + \alpha s)^{1/k}} C_T\right) \quad (25)$$

$$\delta U_{ij} = (U_i - U_j) \frac{A_{overlap}}{A_0} \quad (26)$$

$$\delta U_n = \sqrt{\sum_{k=1}^{n-1} (\delta U_k)^2} \quad (27)$$

In equation (26), δU_{ij} indicates the speed loss of the i -th upstream wind turbine at the j -th downstream wind turbine location, $A_{overlap}$ indicates the intersection area of the i -th upstream wind turbine wake area and the j -th downstream wind turbine rotor area, A_0 indicates the downstream wind turbine rotor area, δU_n indicates the wake loss of the upstream $n - 1$ wind turbines combined effect at the downstream n -th wind turbine, U_n indicates the wind speed at the n -th wind turbine.

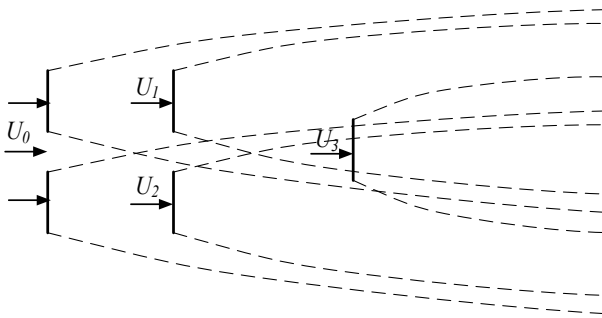


Figure 8. The model of wind farm wake

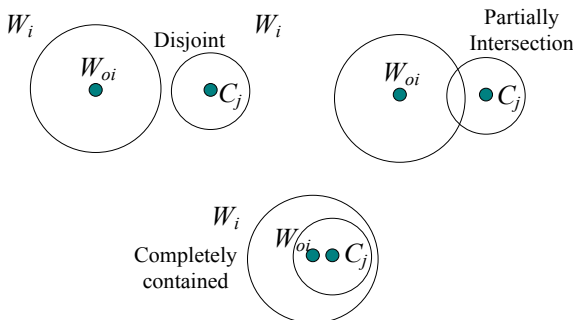


Figure 9. The superposition type wind farm wake

V. INSTANTANEOUS WIND SPEED SPATIAL DISTRIBUTION IN WAKE REGION

According to the wake model described above, the wind farm wake shown in Figure 2 is calculated. Figure 10 shows the wake average velocity profile when the Y coordinates values is 2732 m. In the figure, the wake average velocity reaches a minimum near the coordinate point (544, 2732), because there is a wind turbine in the coordinate point (544, 2732). At the same time, because of the wind turbine wake at the point of (1325, 2921) and the wind turbine wake at (544, 2732) intersect each other at

near 4000 m, the wake average velocity decrease phenomenon appears, the wake superposition phenomenon is formed.

In the wake region, the instantaneous wind speed spatial distribution is mainly affected by the turbulence intensity of its own [18]. Therefore, the Kaimal spectrum of fluctuating wind speed can be obtained according to the equation (3). Then the corresponding fluctuating wind speed spatial distribution can be obtained according to the Kaimal spectrum in wake zone. Figure 11 is a comparison chart about the wake average wind speed and the instantaneous wind speed spatial distribution in wake region. Where the dotted line indicates the wake average wind speed and the solid line represents the spatial distribution of the instantaneous wake wind speed. The figure shows that the spatial distribution of the instantaneous wake wind speed not only describe the wind speed in wake region affected by the wake effect, but also describes the instantaneous wind speed spatial distribution in wake region, it has practical significance for the optimal control of wind turbine.

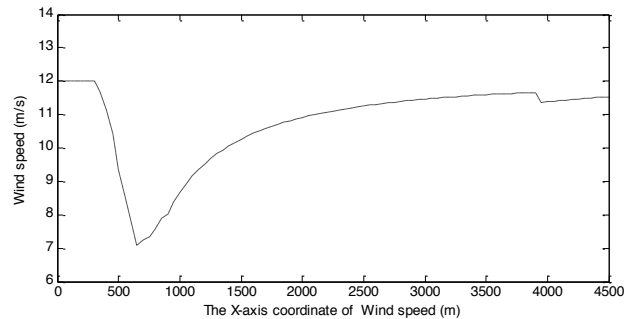


Figure 10. Wake velocity profile

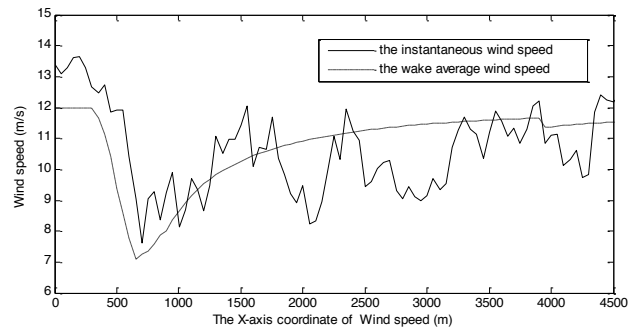


Figure 11. Wind speed distribution in flow field

VI. CONCLUSIONS

The calculation method of instantaneous wind speed spatial distribution for wind farm has been proposed in this paper. This method has divided the instantaneous wind speed spatial distribution of the wind farm into non-wake area and wake area and calculated respectively. For non-wake area, the cross spectral matrix was constructed including the wind turbine mutual distance and the azimuth in the wind farm, and the solving calculation process of the cross spectral matrix was deduced. For wake area, single wind turbine wake model and wake superposition model were established according to conservation of momentum, and then the average wind speed spatial distribution in wake zone was calculated. According to the average wind speed spatial distribution, instantaneous wind speed spatial distribution was obtained. Making a simula-

tion analysis of this method, the results show that the calculation method of instantaneous wind speed spatial distribution for wind farm this paper described can calculate the flow field spatial distribution of wind farm accurately and fast.

ACKNOWLEDGMENTS

When we are in the process to complete this work, we got the help of colleagues, thanks.

REFERENCES

- [1] R. Krishnamurthy, A. Choukulkar, R. Calhoun, et al. Coherent Doppler Lidar for Wind Farm Characterization [J]. *Wind Energy*, 2012, 16(2):189-206. <http://dx.doi.org/10.1002/we.539>
- [2] F. Bingöl. Complex Terrain and Wind Lidars [D]. Denmark: Technical University of Denmark, 2009.
- [3] W. Tian, A. Ozbay, W. Yuan, et al. An Experimental Study on the Performances of Wind Turbines over Complex Terrain [A]. 51st AIAA Aerospace Sciences Meeting including the New Horizons Forum and Aerospace Exposition, 2013.
- [4] E. S. Politis, J. Prospathopoulos, D. Cabezón, et al. Modeling Wake Effects in Large Wind Farms in Complex Terrain: the Problem, the Methods and the Issues [J]. *Wind Energy*, 2012, 15:161-182. <http://dx.doi.org/10.1002/we.481>
- [5] J. M. Prospathopoulos, E. S. Politis, P. K. Chaviaropoulos. Modeling Wind Turbine Wakes in Complex Terrain [A]. EWEC2008, 2008.
- [6] Naeem Memon. Wind Resource Assessment in Complex Terrain Using CFD [D]. Denmark: Technical University of Denmark, 2005.
- [7] D. Cabezón, K.S. Hansen, R.J. Barthelmie. Analysis and Validation of CFD Wind Farm Models in Complex Terrain [A]. EWEC2010, 2010.
- [8] Myungsung Lee, Seung Ho Lee, Nahmkeon Hur, et al. a Numerical Simulation of Flow Field in a Wind Farm on Complex Terrain [A]. APCWE2009, 2009.
- [9] M. Shinozuka. Digital Simulation of Random Processes and its Applications [J]. *Journal of Sound and Vibration*, 1972, 25(1):111-128. [http://dx.doi.org/10.1016/0022-460X\(72\)90600-1](http://dx.doi.org/10.1016/0022-460X(72)90600-1)
- [10] Z. D. Xu, D. X. Wang, K. Y. Wu. Simulation of Stochastic Wind Field for Large Complex Structures based on Modified Fourier Spectrum [J]. *Journal of Zhejiang University-SCIENCE A*, 2011, 12(3):238-246. <http://dx.doi.org/10.1631/jzus.A1000209>
- [11] Jakob Mann. Wind Field Simulation [J]. *Probabilistic Engineering Mechanics*, 1998, 13(4):269-282. [http://dx.doi.org/10.1016/S0266-8920\(97\)00036-2](http://dx.doi.org/10.1016/S0266-8920(97)00036-2)
- [12] L. Kristensen, N. O. Jensen. Lateral Coherence in Isotropic Turbulence and in the Natural Wind [J]. *Boundary Layer Meteorology*, 1979. <http://dx.doi.org/10.1007/BF00117924>
- [13] Y. L. He, H. Liu, J. Du, et al. Simulation Study of Stochastic Fluctuating Wind Field for MW Class WTGS [J]. *Acta energiae solaris sinica*, 2010, 31(2):216-221.
- [14] G. L. He. Wind Field Simulation of the Wind Turbine System [J]. *Proceedings of the CSEE*, 2009, 29(29):108-112.
- [15] W. He, D. Tian, Y. Deng, et al. Turbulent Wind Field Simulation of Wind Turbines with Rotational Effects [J]. *Proceedings of the CSEE*, 2013, 33(11):82-87.
- [16] G. L. He, J. Li. Rotationally Sampled Spectrum of Wind Turbine Tower System Based on Physical Mechanism [J]. *Proceedings of the CSEE*, 2009, 29(26):85-91.
- [17] Paul S. Veers. Three-Dimensional Wind Simulation [J]. Sandia Report, 1988.
- [18] G. Espana, S. Aubrun, S. Loyer. Wind Tunnel Study of the Wake Meandering Downstream of a Modelled Wind Turbine as an Effect of Large Scale Turbulent Eddies [J]. *Journal of Wind Engineering and Industrial Aerodynamics*, 2012, 101: 24-33. <http://dx.doi.org/10.1016/j.jweia.2011.10.011>

AUTHORS

Gu Bo received the Master degree in North China University of Water Resources and Electric power in 2006. Currently, he is a lecturer at North China University of Water Resources and Electric power, School of Electric Power. His interests are in new energy generation technologies. (e-mail: gb19820915@163.com).

Hu Hao, Huang Hui and **Liu Xinyu** are with North China University of Water Resources and Electric power in 2006. Currently, he is a lecturer at North China University of Water Resources and Electric power, School of Electric Power.

The work is supported by National Science and Technology Major Project 863 in china (SQ2010AA0523193001). Submitted 10 September 2014. Published as resubmitted by the authors 25 January 2015.